Available online at www.sciencedirect.com
ScienceDirect
Ceramics International 36 (2010) 561–566
CERAMICS INTERNATIONAL
www.elsevier.com/locate/ceramint

Nanocrystalline yttria stabilized zirconia by metal–PVA complexation

Prasanta K. Ojha [a,b,*], S.K. Rath [a], T.K. Chongdar [a], A.R. Kulkarni [b]

[a] Naval Materials Research Laboratory, Addl Ambernath, Thane 421506, India
[b] Indian Institute of Technology Bombay, Mumbai, India

Received 7 July 2009; received in revised form 24 July 2009; accepted 19 September 2009
Available online 29 October 2009

Abstract

Nanocrystalline 8 mol% yttria stabilized zirconia (YSZ) powder was synthesized using polyvinyl alcohol (PVA) as organic precursor and acidic solutions of yttrium oxynitrite and zirconium nitrate. Complex formation was established using Fourier transform infrared (FTIR) spectroscopy and solid state ^{13}C nuclear magnetic resonance (NMR) spectroscopy. Thermal stability of the complex was investigated by thermogravimetric analysis (TGA). X-ray diffractometry (XRD) revealed formation of cubic phase YSZ at a temperature as low as 600 °C. The lattice parameter and average crystallite size were calculated from the XRD data. Particle size of the YSZ powder was investigated through transmission electron microscopy (TEM). The band gap of the sintered YSZ pellet was measured by UV–Vis-diffused reflectance spectroscopy (DRS). AC electrical conductivity was measured in air at 1 kHz frequency using a programmable RCL meter. The activation energy was calculated from the conductivity data at different temperatures using the standard Arrhenius equation.

Keywords: A. Precursors: organic; Nanocrystalline; YSZ

1. Introduction

Face centered cubic yttria stabilized zirconia (YSZ) finds application in solid oxide fuel cell (SOFC), electrochemical devices such as oxygen sensors and oxygen pumps, due to their excellent performance in terms of thermal stability, chemical stability and oxygen-ion conductivity at moderate to high temperatures [1–5]. YSZs are also used for thermal barrier coatings [6] and optical applications [7]. Various techniques, namely sol–gel method [8], spray pyrolysis [9], RF sputtering [10], reactive magnetron co-sputtering [11], chemical vapor deposition [12], electrochemical vapor deposition [13], plasma spraying [14] and slurry coating [15] have been reported for making homogeneous and impervious YSZ films with desired properties. YSZ powders synthesized by wet chemical methods usually have very narrow particle size distribution and fine grains. The FCC phase of YSZ powder also forms at low temperature and provides better functional properties in many cases [16–26]. In wet chemical synthesis of ceramic powders via organic precursors reduces the possibility of agglomerate formation. This is due to the primary oxide particles formed during initial stages of calcinations are shielded and kept separated by the organic groups from neighboring oxide particles.

In this work, we have adopted a simple approach to synthesize nanometer-size YSZ powder. Wherein, metal oxides have been synthesized through an intermediate complex, formed as a result of the reaction between polyvinyl alcohol (PVA) and mixture of zirconium and yttrium metal solution. Normally, PVA is considered as a stable polymer, but it was observed that in acidic conditions (at a pH ∼2) it reacts with a mixture of zirconium oxynitrite and yttrium nitrate (in 92:8 molar ratios) to form a metal–PVA complex. The complex formed was characterized by Fourier transform infrared (FTIR) spectroscopy and solid state ^{13}C nuclear magnetic resonance (NMR) spectroscopy. Thermal stability of the metal–PVA complex was investigated via thermogravimetric analysis (TGA). Phase formations on calcinations at different temperatures were investigated through X-ray diffractometry (XRD). Lattice parameters and crystallite size were calculated from XRD data. Grain sizes of the YSZ powders were determined using transmission electron microscopy (TEM). The sintering behavior of the powders was studied by making pellets of these powders

* Corresponding author at: Naval Materials Research Laboratory, Addl Ambernath, Thane 421506, India.
E-mail address: pkojha77@yahoo.co.in (P.K. Ojha).

0272-8842/$36.00
doi:10.1016/j.ceramint.2009.09.035

via uniaxial pressing in a hydraulic press and subsequent sintering in air in a bottom loading furnace. Band gap of YSZ pellet was measured by UV–Vis-diffused reflectance spectroscopy (DRS). Electrical property of the YSZ pellet was measured by impedance analysis at different temperatures and frequencies. From the conductivity data the activation energy was calculated using standard Arrhenius equation.

2. Experimental

Zirconium oxychloride ($ZrOCl_2{\cdot}8H_2O$, 99.9% purity) and yttrium oxide (Y_2O_3, 99.9% purity) were purchased from Indian Rare Earth Ltd. and used as received. 98% hydrolyzed polyvinyl alcohol (MW 89,000–98,000) from Sigma–Aldrich, USA, AR grade nitric acid from Merck, and deionized water were used for the synthesis work. Fig. 1 shows the flow chart of the synthesis process. Oxynitrite solution (pH ≈2) of zirconium was prepared by dissolving zirconium oxychloride in concentrated HNO_3 in a ratio of 1:4 (w/v) and heated at 60 °C to make it Cl_2 free. To prepare yttrium nitrate solution, yttrium oxide was directly dissolved in concentrated HNO_3 in a ratio of 1:20 (w/v). The metal content per unit volume of both the solutions was evaluated by treating the metal nitrate with mandelic acid. Metal nitrate reacts with mandelic acid at a temperature of 60 °C to form a mandalate complex that precipitates out. The precipitated metal complex was filtered and roasted at 1000 °C to form the metal oxide from which the metal amount can be calculated. Metal estimation was carefully carried out as it is very useful for preparation of stoichiometric composition. 5% PVA solution was prepared by dissolving requisite amount of PVA granules in deionized water. For preparing 8 mol% YSZ, 0.92 molar $Zr(ONO_2)_4$ and 0.16 molar $Y(NO_3)_3$ solution were taken in a glass beaker. The beaker was kept on a hot plate at 90 °C. PVA solution was added drop wise to the nitrate bath with constant stirring. Initiation of complex formation was indicated by evolution of NO_x fumes with the solution simultaneously turning turbid (due to precipitation of complex). The metal–PVA complexation process was completed within an hour. The powders were collected by filtration

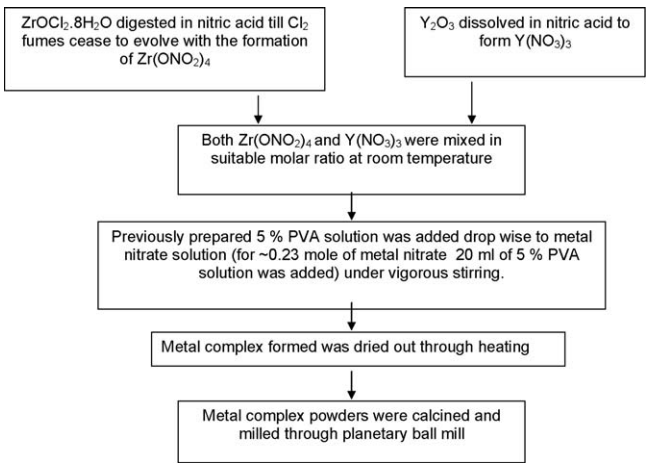

Fig. 1. Flow chart of the synthesis procedure of YSZ powders from metal precursors.

and dried at 60 °C in an oven. A 1600 Series FTIR (Perkin-Elmer, USA) was used to characterize both PVA and the metal complex using KBr pellet method. Solid state ^{13}C NMR spectra of the samples were acquired at 125 MHz using a Bruker Avance-500 NMR spectrometer and a high resolution 4 mm CP/MAS probe. Thermo gravimetric analysis (Model: Setsys 16, SETARAM, France) was carried out in air to find out the decomposition temperature of the organo-metallic complex. The metal complex powders were then heat treated at 600, 700 and 800 °C for 1 h in air. X-ray diffractometry (XPert MPD, PAnalytical) was carried out for the as prepared metal–PVA complex powder and the heat treated powders for phase identification. Cu Kα radiation in the range of 20–80° (2θ) with a step size of 0.005° was used for diffractometry. The XRD patterns were subsequently processed by eliminating $K\alpha_2$, subtracting background and nominal smoothening by fast Fourier method. The peaks were identified and indexed. FWHM data were used for estimation of crystallite size using the Scherer's formula. YSZ powders dispersed in a Cu grid were characterized through transmission electron microscopy (Philips, USA) to estimate the grain size.

The YSZ powders after calcination at 800 °C were ball milled for 2 h in a planetary ball mill using ethanol, to break the agglomerates. The powders were dried and sieved for pelletisation. Pellets were prepared by uniaxial pressing of loose powders in a steel mould under a pressure of 5000 MPa. The pellets were then sintered in a bottom loading furnace in air at 1600 °C. Density of the sintered samples was measured using Archimedes principle. Band gap was measured by diffused reflectance spectroscopy (DRS) using UV–Vis-DRS Spectrometer (Labsphere, Model No. DRA-CA-5500 and Cary 500 scan, Varian) in the wavelength range of 200–800 nm. Microstructure of the polished and thermally etched surface of the sintered pellet was observed under scanning electron microscope (LEO 1455, UK). AC electrical conductivity of the sintered pellet at different temperatures and frequencies was measured using PM 6304, programmable RLC meter, Philips, Germany and platinum as electrodes. For high temperature impedance analysis, the sample holder was kept inside a table top model furnace and attached to the impedance analyzer through platinum wire. The activation energy was calculated from the conductivity data at high temperatures. According to the standard Arrhenius equation, plot of log conductivity vs. 1000/T gave a straight line with a negative slope, from which activation energy was calculated.

3. Results and discussion

The complexation process is initiated with the evolution of brown NO_x fumes; however, the completion is indicated by cessation of evolution of brown fumes upon further addition of PVA. Formation of complex has been confirmed by FTIR and solid state ^{13}C NMR.

FTIR spectra of PVA and metal–PVA complex are shown in Fig. 2. Appearance of the characteristic Zr–O–C peak at 809 cm^{-1} and the strong suppression of peak due to C–O–H bond at 3355 cm^{-1} confirm the occurrence of complexation reaction

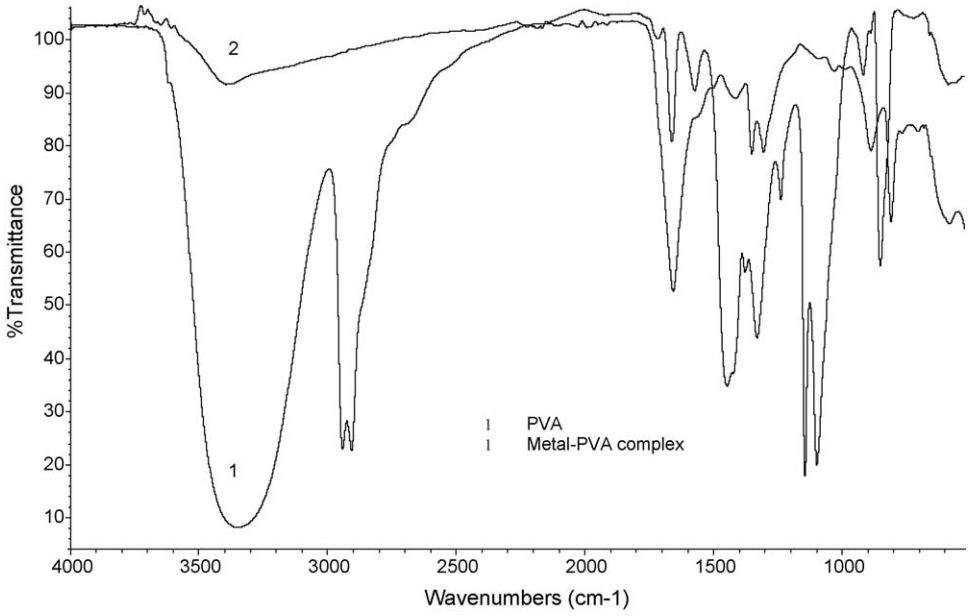

Fig. 2. FTIR spectra of 1. PVA, 2. metal–PVA complex.

via formation of Zr–PVA bond. Solid state ^{13}C NMR spectra of PVA and metal–PVA complex are shown in Fig. 3. NMR results reveal a drastic change in the spectra on complexation. Peaks at 76.75 (s), 70.99 (s), 67.17 (s), 65.35 (s) and 45.14 (s) ppm corresponding to the neat PVA are absent while a new peak at 170.94 (s) ppm is observed in the spectrum of the complex. Similar observation has been reported by Podsiadlo et al. [27] in complexation of PVA with montmorillonite, which suggests formation of complex in this case as well.

Fig. 4 shows the TGA plot of the complex. Initial weight loss in the trace at about 100 °C is primarily due to moisture present due to hygroscopic character of PVA. The second discontinuity in the trace appears at 300 °C indicating decomposition of specific groups of the zirconium–PVA complex, however, the total decomposition of zirconium–PVA takes place at the third discontinuity in the plot, at about 380 °C. Finally, the yttrium–PVA complex decomposes to oxides at 610 °C. The experimental value matches well with the calculated value when it is presumed that all metal–PVA complexes decompose to metal oxide with H_2O and CO_2 as the volatile products.

XRD analysis of the samples, calcined at various temperatures, is shown in Fig. 5. Minimum calcination temperature employed was 600 °C since, as per DTA results the complex decomposed completely beyond 610 °C. XRD results show the formation of phase pure FCC YSZ even at a temperature as low as 600 °C. The peaks were identified and properly indexed by comparing with the JCPDS value. Lattice parameter was calculated from the peak data and found to be 5.12 Å, which is in good agreement with the reported value [28]. The average crystallite size was calculated by Scherer's method, using FWHM of most intense peaks, and found to be about 35 nm. This is also in good agreement with the result

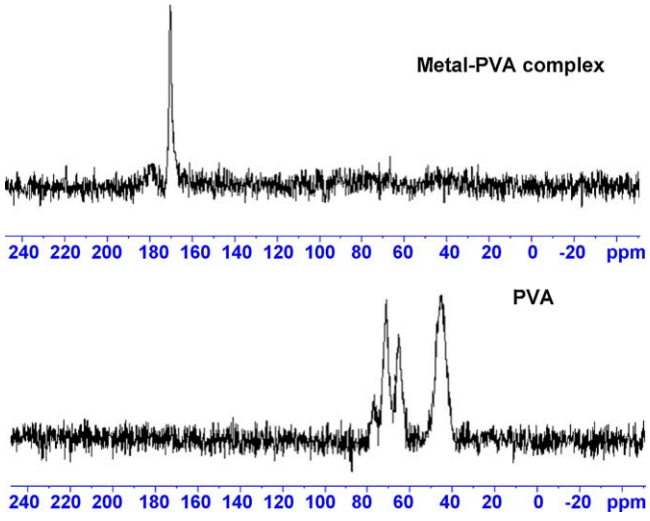

Fig. 3. ^{13}C NMR of PVA and metal–PVA complex.

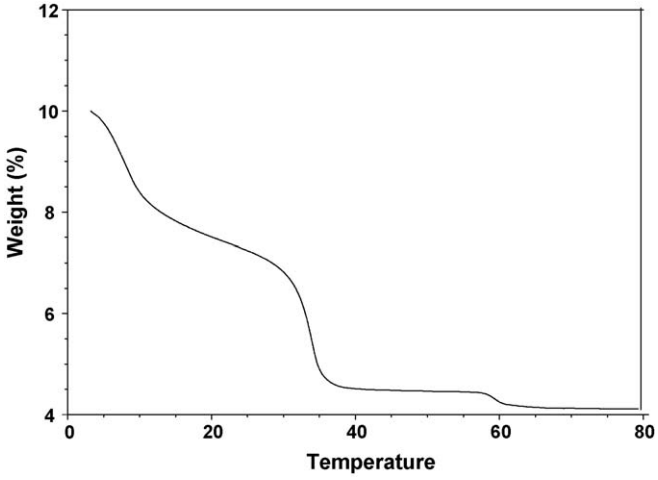

Fig. 4. Thermo gravimetric analysis of the metal–PVA complex.

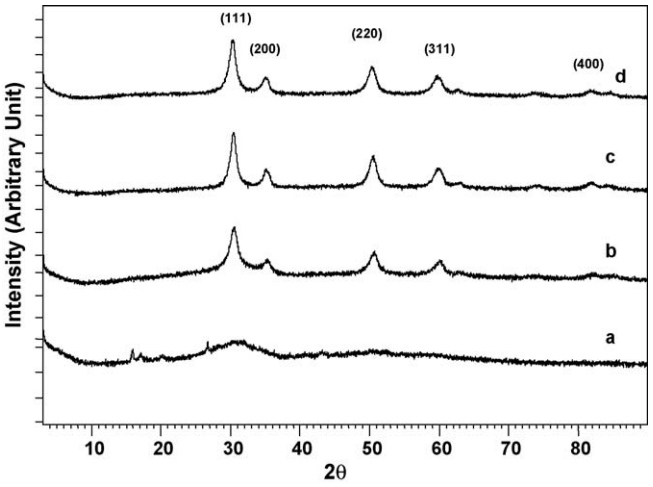

Fig. 5. X-ray diffraction analysis of the sample calcined at different temperature (a) as prepared sample without calcined, (b) calcined at 600 °C, (c) calcined at 700 °C and (d) calcined at 800 °C.

obtained by dark field transmission electron microscopy of the powder samples heat treated at 800 °C, as shown in Fig. 6. The TEM image analysis clearly indicates uniform grain size of about 30–50 nm. As the average crystallite size calculated from XRD data is similar to the average grain size observed in TEM, it may be inferred that the oxide particles obtained after calcination are single crystallites. Uniaxially pressed pellets were sintered in air at 1600 °C and maximum density of the sintered YSZ pellet was found out to be 5.6×10^3 kg/m^3 which is approximately 95% of the theoretical density. A lower value than the theoretical density could be due to the presence of micropores in the sintered matrix as observed in the SEM micrograph (Fig. 7) of the polished and thermally etched

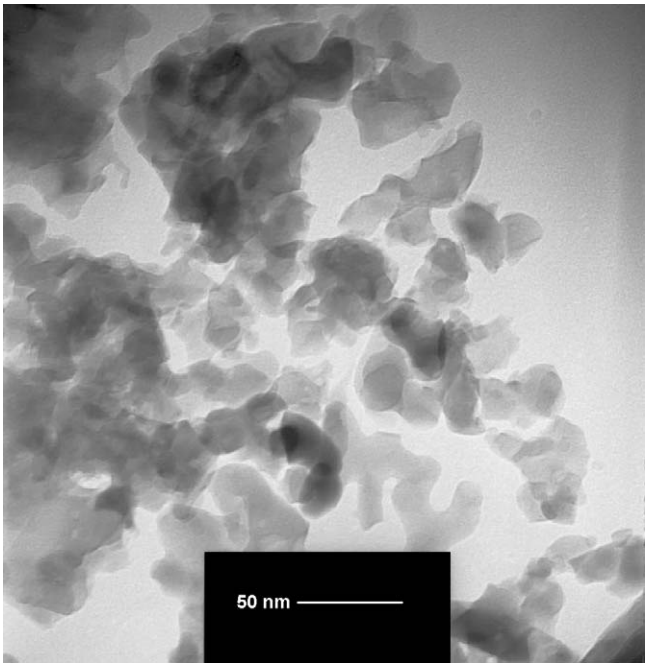

Fig. 6. Dark field TEM image of $(ZrO_2)_{0.92}(Y_2O_3)_{0.08}$ powder.

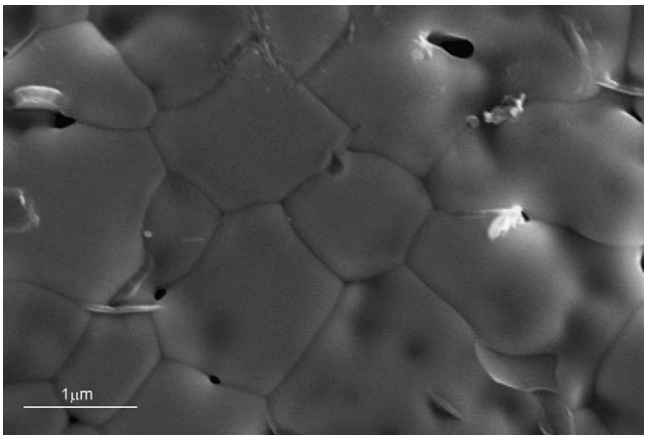

Fig. 7. SEM photograph of the polished and thermally etched surface of sintered pellet.

surface of the sintered sample. Further, nanosized powders have an agglomerating tendency which might also result in lower sintering density.

UV–Vis-diffused reflectance spectroscopy of the synthesized 8 mol% YSZ is shown in Fig. 8. The onset point of absorption which corresponds to the electronic excitation is 303 nm. This wavelength corresponds to a band gap of 4.1 eV, which is close to the reported values [29,30]. Such a high band gap makes the material an electrical insulator which is one of the desired characteristics for SOFC electrolyte. 8YSZ synthesized by citrate–nitrate gel combustion process reported in our previous work [31], exhibited a band gap of 2.99 eV.

AC conductivity of the 8 mol% YSZ sintered pellet was measured at different temperatures at 1 kHz frequency. Fig. 9 shows the conductivity plot of the pellet at different temperatures. Nature of the plot indicates a typical thermal diffusion curve. This may be explained by the diffusion of oxide ions across the pellet under an applied electric field. The conductivity of the sintered pellet at 1000 °C was found to be 0.12 S cm^{-1}, which is in good agreement with the reported value of 8YSZ conductivity synthesized by solid state route [1,32,33]. However, Patil et al. [26] have reported a conductivity value of 0.098 S cm^{-1} for the YSZ powders synthesized by organic precursor route. Thus the present wet

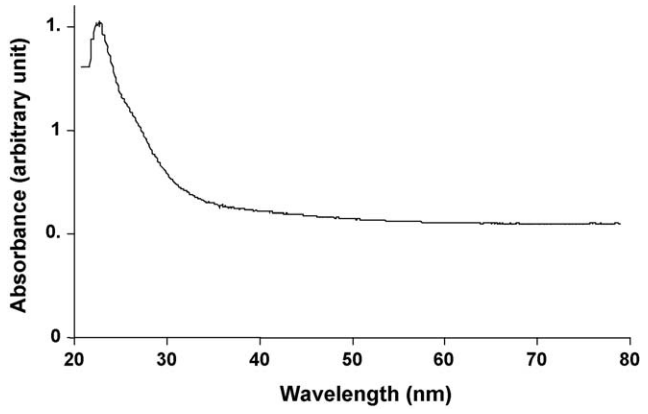

Fig. 8. UV-DRS measurement of $(ZrO_2)_{0.92}(Y_2O_3)_{0.08}$ nanocrystallite powder.

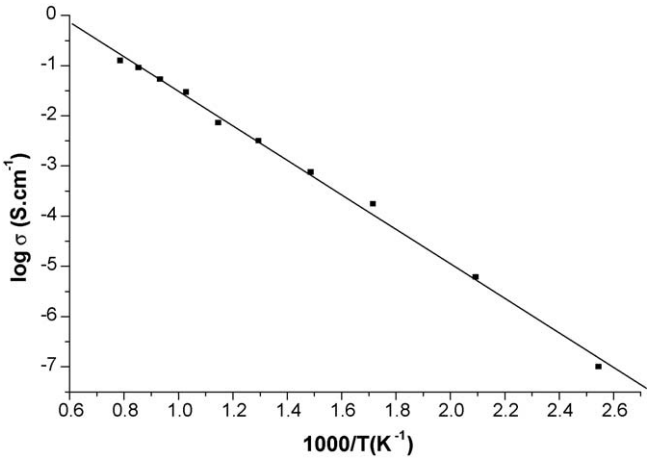

Fig. 9. Conductivity measurement of $(ZrO_2)_{0.92}(Y_2O_3)_{0.08}$ at different temperature.

chemical approach is found to be advantageous in synthesis of YSZ powders with higher band gap and AC conductivity value.

From the conductivity plot, activation energy for diffusion was calculated using the standard Arrhenius equation and found to be 65 kJ (equivalent to 0.68 eV). The activation energy found to be low compared to the reported value of 1.13 eV [34], which gives an additional advantage of this synthesis process.

4. Conclusion

Nanocrystalline 8 mol% YSZ powders have been synthesized using a very simple method of complex formation between metal oxynitrite and PVA. The complexation process is confirmed by FTIR and ^{13}C NMR techniques. The metal–PVA complex, on calcination at 600 °C in air, transforms to phase pure FCC YSZ with lattice parameter 5.12 Å. The average crystallite size was 35 nm. TEM image of the YSZ powder showed grains with an average grain size of 30–50 nm. 95% of the theoretical density could be achieved for pellets on sintering at 1600 °C. UV–Vis-DRS results measured a band gap of 4.1 eV for the sintered YSZ pellet. A high band gap and a high AC electrical conductivity at 1 kHz (0.12 S cm^{-1} at 1000 °C) together with low activation energy (0.68 eV) makes it an acceptable material for SOFC electrolyte.

Acknowledgements

The authors wish to acknowledge the persons associated with the TEM facility at SAIF, IIT Bombay, for providing necessary help to do TEM characterization of the samples. We are thankful to TIFR, Mumbai for providing assistance in carrying out the solid state ^{13}C NMR of our samples.

References

[1] N.Q. Minh, Ceramic fuel cell, J. Am. Ceram. Soc. 76 (1993) 563–588.
[2] B.C.H. Steele, Material science and engineering: the enabling technology for the commercialization of fuel cell systems, J. Mater. Sci. 36 (2001) 1053–1068.
[3] M.L. Perry, T.F. Fuller, A historical perspective of fuel cell technology in the 20th century, J. Elctron. Chem. Soc. 149 (2002) 559–567.
[4] H. Feuer, J. Margalit, SOFCs—too hot to handle? J. Am. Ceram. Soc. Bull. 83 (2004) 12–15.
[5] T. Fukui, K. Murata, S. Ohara, H. Abe, M. Naito, K. Nogi, Morphology control of Ni–YSZ cermet anode for lower temperature operation of SOFCs, J. Power Sources 125 (2004) 17–21.
[6] M. Leoni, R.L. Jones, P. Scardi, Phase stability of scandia–yttria-stabilized zirconia TBCs, Surf. Coat. Technol. 108–109 (1998) 107–113.
[7] I. Kosacki, V. Petrovsky, H.U. Anderson, Band gap energy in nanocrystalline ZrO_2:16% Y thin films, Appl. Phys. Lett. 74 (1999) 341–343.
[8] C.R. Xia, H.Q. Cao, H. Wang, P.H. Yang, G.Y. Meng, D.K. Peng, Sol–gel synthesis of yttria stabilized zirconia membranes through controlled hydrolysis of zirconium alkoxide, J. Membr. Sci. 162 (1999) 181–186.
[9] Y. Matsuzaki, M. Hishinuma, I. Yasuda, Growth of yttria-stabilized zirconia thin films by metallo-organic, ultrasonic spray-pyrolysis, Thin Solid Films 340 (1999) 72–76.
[10] B Gharbage, F. Mandier, H. Lauret, C. Roux, T. Pagnier, Electrical properties of $La_{0.5}Sr_{0.5}MnO_3$, Solid State Ionics 82 (1) (1995) 85–94.
[11] S. Horita, M. Watanabe, S. Umemoto, A. Masuda, Material properties of heteroepitaxial yttria-stabilized zirconia films with controlled yttria content on Si prepared by reactive sputtering, Vacuum 51 (1998) 609–613.
[12] H.B. Wang, C.R. Xia, G.Y. Meng, D.K. Peng, Deposition and characterization of YSZ thin films by aerosol-assisted CVD, Mater. Lett. 44 (2000) 23–28.
[13] T. Ioroi, T. Hara, Y. Uchimoto, Z. Oguchi, Z. Takehara, Preparation of Perovskite-type $La_{1-x}Sr_xMnO_3$ films by vapour-phase processes and their electrochemical properties, J. Electrochem. Soc. 144 (1997) 1362–1370.
[14] G. Chiodelli, A. Magistris, M. Scagliotti, F. Parmagiani, Electrical properties of plasma-sprayed yttria-stabilized zirconia films, J. Mater. Sci. 23 (1988) 1159–1163.
[15] J. Will, Diss, Porous support structures and sintered thin film electrolytes for solid oxide fuel cells, ETH No. 12876, ETH, Zurich, 1998.
[16] O. Vasylkiv, Y. Sakka, Nonisothermal synthesis of yttria-stabilized zirconia nanopowder through oxalate processing: I. Characteristics of Y–Zr oxalate synthesis and its decomposition, J. Am. Ceram. Soc. 83 (2000) 2196–2202.
[17] O. Vasylkiv, Y. Sakka, H. Borodians'ka, Nonisothermal synthesis of yttria-stabilized zirconia nanopowder through oxalate processing: II. Morphology manipulation, J. Am. Ceram. Soc. 84 (2001) 2484–2488.
[18] X. Wang, J. Zhuang, Q. Peng, Y. Li, A general strategy for nanocrystal synthesis, Nature 71 (2005) 121–124.
[19] C.L. Ong, J. Wang, S.C. Ng, L.M. Gan, Effect of chemical species on the crystallization behavior of sol derived zirconia precursor, J. Am. Ceram. Soc. 81 (1998) 2624–2628.
[20] O. Vasylkiv, Y. Sakka, Synthesis and colloidal processing of zirconia nanopowders, J. Am. Ceram. Soc. 84 (2001) 2489–2494.
[21] R.E. Juarez, D.G. Lamas, G.E. Lascalea, N.E.W. Reca, Synthesis of nanocrystalline zirconia powders for TZP ceramics by nitrate–citrate combustion route, J. Eur. Ceram. Soc. 20 (2000) 133–138.
[22] J.C. Ray, R.K. Pati, P. Pramanik, Chemical synthesis and structural characterization of nanocrystalline powders of zirconia and yttria stabilized zirconia (YSZ), J. Eur. Ceram. Soc. 20 (2000) 1289–1295.
[23] S.K. Saha, P. Pramanik, Innovative chemical method for preparation of calcia stabilized zirconia powders, Br. Ceram. Trans. 94 (1995) 123–127.
[24] E. Mustafa, M. Wilhelm, W. Wruss, Microstructure and phase stability of Y–PSZ co doped with MgO or CaO prepared via polymeric route, Br. Ceram. Trans. 101 (2002) 78–83.
[25] T. Yoshioka, K. Dosaka, T. Sato, A. Okuwaki, S. Tanno, T. Miura, Preparation of spherical ceria doped tetragonal zirconia by the spray pyrolysis method, J. Mater. Sci. Lett. 11 (1992) 51–55.
[26] D.S. Patil, et al., Eight mole percent yttria stabilized zirconia powders by organic precursor route, Ceram. Int. 34 (5) (2008) 1195–1199.
[27] P. Podsiadlo, et al., Ultrastrong and stiff layered polymer nanocomposite, Science 318 (2007) 80–83.
[28] R.P. Ingel, D. Lewis III, Lattice parameters and density for Y_2O_3-stabilized ZrO_2, J. Am. Ceram. Soc. 69 (4) (1986) 325–332.

[29] V.R. PaiVernker, A.N. Peteline, F.J. Crowne, D.C. Nagale, Colour center induced band gap shift in yttria-stabilised zirconia, Phys. Rev. B 40 (12) (1989) 8555–8557.
[30] I. Kosacki, V. Petrovosky, H.U. Anderson, Band gap energy in nanocrystalline ZrO_2–16% Y thin films, Appl. Phys. Lett. 74 (3) (1999) 341–343.
[31] M. Biswas, K. Shashidhara, P.K. Ojha, T.K. Chongdar, N. Ratan Bandyopadhyay, Linear combination of atomic orbitals approximation in nanocrystalline yttria-stabilized zirconia synthesized by citrate–nitrate gel combustion process, J. Am. Ceram. Soc. 91 (3) (2008) 934–937.
[32] T.H. Etsell, S.N. Flengas, The electrical properties of solid oxide electrolytes, Chem. Rev. 70 (1970) 339–376.
[33] S.C. Singhal, K. Kendall, High Temperature Solid Oxide Fuel Cells Fundamentals, Design and Applications, Elsevier Ltd., 2003 ISBN 1856173879.
[34] G.C.T. Silva, E.N.S. Muchillo, Electrical conductivity of yttria-stabilized zirconia with cobalt addition, Solid State Ionics 180 (11–13) (2009) 835–838.